

Decoherence as a probe of coherent quantum dynamics

Michael B. d'Arcy,¹ Rachel M. Godun,¹ Gil S. Summy,^{1,2} Italo Guarneri,^{3,4,5} Sandro Wimberger,^{4,5,6} Shmuel Fishman,⁷ and Andreas Buchleitner⁶

¹*Clarendon Laboratory, Department of Physics, University of Oxford, Parks Road, Oxford OX1 3PU, United Kingdom*

²*Department of Physics, Oklahoma State University, Stillwater, Oklahoma 74078-3072, USA*

³*Università degli Studi dell'Insubria, Via Valleggio 11, I-22100 Como, Italy*

⁴*Instituto Nazionale per la Fisica della Materia, Unità di Milano, Via Celoria, I-20133 Milano, Italy*

⁵*Instituto Nazionale di Fisica Nucleare, Sezione di Pavia, Via Bassi 6, I-27100 Pavia, Italy*

⁶*Max-Planck-Institut für Physik Komplexer Systeme, Nöthnitzer Strasse 38, D-01187 Dresden, Germany*

⁷*Physics Department, Technion, Haifa IL-32000, Israel*

(Received 5 July 2003; published 26 February 2004)

The effect of decoherence, induced by spontaneous emission, on the dynamics of cold atoms periodically kicked by an optical lattice is experimentally and theoretically studied. Ideally, the mean energy growth is essentially unaffected by weak decoherence, but the resonant momentum distributions are fundamentally altered. It is shown that experiments are inevitably sensitive to certain nontrivial features of these distributions, in a way that explains the puzzle of the observed enhancement of resonances by decoherence [Phys. Rev. Lett. **87**, 074102 (2001)]. This clarifies both the nature of the coherent evolution, and the way in which decoherence disrupts it.

DOI: 10.1103/PhysRevE.69.027201

PACS number(s): 05.45.Mt, 03.65.Yz, 32.80.Lg, 42.50.Vk

The theory of coherent quantum transport in periodic potentials is basic to solid state physics, and to our understanding of various conductance phenomena in crystal lattices. After succeeding in isolating and manipulating single quantum objects such as ions or atoms, quantum opticians, as well as meso- and nanoscientists, have now started to build extended structures of atoms or ions of increasing complexity. A natural way of doing so is to arrange one, two, or three dimensional regular arrays of (cold or ultracold) atoms in optical lattices [1], which then can be considered as faithful realizations of strongly idealized, fundamental models of solid state theory. Beyond illustrating such theoretical models under clean and virtually perfectly controlled laboratory conditions, these experiments often also hold unexpected surprises (due to apparently innocent, real-life modifications of the original model), and promise highly rewarding technical applications in the future. Proposals that suggest using optical lattices for quantum information processing [2] are but one example of this.

In all such respects, the impact of noise and decoherence is a crucial issue [3–5], because decoherence is expected to impair manifestly quantum phenomena. The present Brief Report addresses a striking, seeming violation of this rule, which was experimentally observed with kicked cold atoms subjected to a pulsed, one-dimensional, spatially periodic optical lattice [6]. Here, a peculiar type of coherent quantum transport, called “quantum resonance” [7,8] is theoretically predicted for kicking periods rationally related to the propagation time of kicked atoms across the lattice constant. The mean kinetic energy of an atomic ensemble is then predicted to increase linearly with time, in sharp contrast to the behavior predicted for nonresonant values of the kicking period, where it saturates (in the process of “dynamical localization” [9], closely analogous to Anderson localization in one-dimensional disordered solids [10]). In previous experiments, enhanced transport was indeed observed for the

lowest-order resonances [6,11]. When decoherence was added to the experiment by controlled spontaneous emission (SE), the energy growth at resonance was found to be significantly faster than could be accounted for by the heating effect of momentum transfer due to SE [6,12]. This looks like incoherent magnification of a purely coherent, and non-classical, phenomenon.

In this Brief Report we show how this counterintuitive effect of decoherence can be resolved by inspection of the full atomic momentum distributions instead of merely their mean square (i.e., kinetic energy) values, as were considered in Ref. [6]. Decoherence then acts as expected: it destroys the coherent dynamics underlying the quantum resonances and, in particular, certain nontrivial features of the momentum distributions [7]. It is precisely this latter fact that produces the surprising enhancement of the mean energy values observed in the experiment [6,7].

Our experimental system [12] is a realization of the paradigmatic kicked rotor (KR) model [9,13], extensively used in investigations of classical chaotic dynamics and its quantum counterpart [14]. After trapping and cooling in a magneto-optic trap, about 10^7 cesium atoms are released and, falling freely under gravity, are exposed to pulses from a vertical standing wave of off-resonant laser light. This is red-detuned from the $6^2S_{1/2} \rightarrow 6^2P_{1/2}$ ($F=4 \rightarrow F'=3$) $D1$ transition by $\delta_L = 2\pi \times 30$ GHz, and has a wavelength $\lambda_L = 894.7$ nm. On release, the atomic temperature is $5 \mu\text{K}$, corresponding to a Gaussian momentum distribution with full width at half maximum (FWHM) $12\hbar k_L$, where $k_L = 2\pi/\lambda_L$. The duration of each (square) pulse is $t_p = 500$ ns, and the peak intensity in the standing wave is $\approx 5 \times 10^4$ mW/cm². Due to the ac Stark shift, these pulses result in δ -function-like applications of a sinusoidal potential, with spatial period $\lambda_L/2$. Classically, the maximum impulse that this can impart is $\hbar G \phi_d$, where $\phi_d = \Omega^2 t_p / 8\delta_L$, and Ω is the Rabi frequency of the atoms at the intensity maxima of the light field. Quan-

tum mechanically, it imparts momentum to the atoms in integer multiples of $\hbar G$, where $G=2k_L$. Both the density distribution of the trapped atoms and the standing light wave intensity profile are Gaussian, each with FWHM 1 mm, so the mean value of ϕ_d as experienced by the atomic ensemble is $\approx 0.8\pi$. The standing wave passes through a voltage-controlled crystal phase modulator which can shift the position of the standing wave between consecutive pulses so that it effectively cancels the effect of gravity. Thus in the rest frame of the atomic ensemble the standing wave appears to be stationary, yielding KR dynamics with kicking period T ($\gg t_p$), despite the presence of gravity. Decoherence can be introduced by inducing SE in the atoms through application of an additional 2 μ s pulse of laser light after each of the kicking pulses. This light is 60 MHz red-detuned from the $6^2S_{1/2} \rightarrow 6^2P_{3/2}$ ($F=4 \rightarrow F''=5$) $D2$ transition. The intensity of the pulse can be controlled so that the mean number of SE per atom per pulsing cycle, \bar{n}_{SE} , can be varied continuously. Finally, after application of the pulses, the atoms fall through a sheet of light resonant with the $D2$ transition, located 0.5 m below the point of release. This allows us to determine their momentum distribution by a time-of-flight (TOF) technique, with a resolution of $\approx \hbar G$.

In the absence of SE, the Hamiltonian that generates the time evolution of the atomic wave function may be written in the following dimensionless form

$$\hat{H}(t) = \frac{\hat{p}^2}{2} + \phi_d \cos(\hat{x}) \sum_{m=-\infty}^{+\infty} \delta(t - m\tau), \quad (1)$$

where p is momentum in units of $\hbar G$, x is position in units of G^{-1} , and M is the mass of the atoms. The units of energy and time are then $\hbar^2 G^2 / M$ and $M / \hbar G^2$, respectively. In such units the kicking period is $\tau = \hbar G^2 T / M$. This Hamiltonian is very close to that of the well-known δ -kicked rotor, with the sole (but important, as discussed below) difference that our cold atoms are moving along a line rather than in a circle. Notwithstanding this, the dynamics of the atoms reflect characteristic properties of the quantum KR (whose corresponding classical phase space is mixed, consisting of regular and chaotic components, for nonvanishing kicking strength [15]). The nature of the quantum transport sensitively depends on the parameter τ . If $\tau = 4\pi r/q$, with r, q integers, then the kicking period is rationally related to the propagation time of kicked atoms across the lattice constant, and quantum transport is typically enhanced by quantum resonance [8]. If $\tau/4\pi$ is sufficiently irrational, then transport is inhibited by quantum interference, i.e., by dynamical localization [9].

A conceptually simple way of experimentally testing this theoretical picture is to measure as a function of τ the mean kinetic energy of the atoms, henceforth to be referred to as ‘‘mean energy,’’ after a fixed interaction time of N kicks. The result of such a measurement at $N=30$ in the absence of SE is shown in Fig. 1(a), with $0.19\pi \leq \tau \leq 6.31\pi$. The mean energies were extracted from a finite momentum window ($-60 \leq p \leq 60$), and low-amplitude noise in the time-of-flight signal was eliminated by imposing a signal threshold estimated from the background noise level at high momenta.

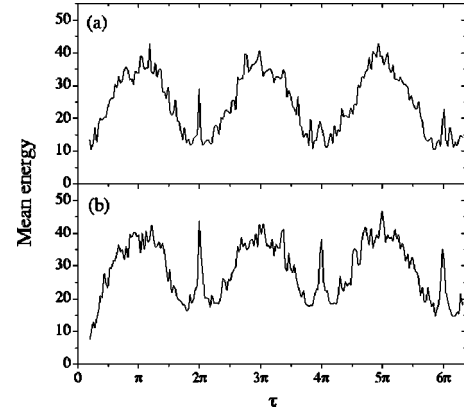


FIG. 1. Experimental values of the mean energy of the atomic ensemble after 30 kicks, as τ is varied from 0.19π to 6.31π (i.e., $6.5 \mu\text{s} \leq T \leq 210.5 \mu\text{s}$) in (a) the absence, and (b) the presence of induced spontaneous emission, with $\bar{n}_{SE} \approx 0.14$.

Figure 1(a) shows an underlying smooth, periodic dependence on τ . This reflects the τ dependence of the localization length of the dynamically localized atomic sample [16]. The structure superimposed on the basic periodic variation has particularly narrow peaks at $\tau=2\pi, 4\pi, 6\pi$. These are the main quantum resonances, with $q=1, r=1$ and $q=2, r=1, 3$. Higher-order ($q \geq 3$) resonances were not unambiguously resolved within the given observation time. The present Brief Report is therefore focused on the main resonances, and specifically at the surprising way in which they react to decoherence, as shown in Fig. 1(b). The mean energy growth at the resonances is clearly enhanced. In other words, resonant transport, which is due to constructive quantum interference, appears to be stabilized by decoherence (while the dynamical localization away from resonance is barely affected, confirming that we are in the regime of weak decoherence [3]). The apparent inconsistency of these experimental observations with what seems theoretically reasonable is resolved as follows.

An atom periodically kicked in space and time is described by a wave packet $\psi(x)$ composed of 2π -periodic Bloch states $\psi_\beta(x)$, that is,

$$\psi(x) = \int_0^1 d\beta \exp(i\beta x) \psi_\beta(x), \quad (2)$$

where β is the quasimomentum. In our units, it is given by the fractional part of the momentum $p = n + \beta$ ($n \in \mathbb{Z}$). It is conserved in time, so the different Bloch states in Eq. (2) evolve independently of one another, and their momenta only change by integers. Under the resonance condition $\tau = 4\pi r/q$, a special situation occurs for a specific, discrete subclass of values of β . Besides being periodic in coordinate space, the one-period evolution (Floquet) operator is then also periodic in momentum space, with the integer period q . This happens when $\beta = m/2r$, $0 \leq m < 2r$, m integer. The amplitudes of such waves at momentum states separated by $q\hbar G$ (in physical units) exactly rephase after each kick [6]; here we specialize to $q=1, 2$. This rephasing is analogous to the Talbot effect in optics, so we speak of these resonances

as occurring at rational multiples of the half-Talbot time $T_{1/2} = 2\pi M/\hbar G^2 = 66.7 \mu\text{s}$ (for which $\tau = 2\pi$). In much the same way as spatial periodicity enforces ballistic motion in physical space, the momentum periodicity which holds for special values of β (i.e., $\beta = 1/2$ for $q = 2$, and $\beta = 0, 1/2$ for $q = 1$) enforces ballistic propagation of the corresponding states in momentum space; thus their energy grows quadratically in time. The remaining Bloch components of the original wave packet, with β not in the “resonant” class, undergo a quasiperiodic energy exchange with the driving field, leading to a finite spread of the associated (β -dependent) momentum distribution for all times. Upon incoherently averaging over the continuous set of quasimomenta which constitute the atomic ensemble, there is competition between quasiperiodic and ballistic propagation, and as N increases the values of β that populate the ballistic growth must match more closely the ideal resonant values. On the one hand, this leads to linear growth of the total mean energy, $E \approx \phi_d^2 N/4$. On the other hand, a stationary momentum distribution $P_s(n) = \lim_{N \rightarrow \infty} P(n, N)$ [7], given by

$$P_s(n) = \sum_{n'} h(n') \int_{-\pi}^{\pi} \frac{d\xi}{2\pi} \int_0^{2\pi} \frac{d\alpha}{2\pi} J_{n-n'}^2(f(\xi, \alpha)), \quad (3)$$

emerges, where $P(n, N)$ is the coarse-grained momentum distribution of the ensemble after N kicks. The coarse graining is on the scale of unity ($\hbar G$ in physical units) so as to yield a distribution in n , which is consistent with the finite-size binning of the experimentally detected momentum distribution. In Eq. (3), $h(n')$ is the initial (assumed smooth) momentum distribution, $f(\xi, \alpha) = \phi_d \sin(\xi) \csc(\alpha)$, $\xi = \pi(2\beta - 1)$, and $J_{n-n'}$ is a Bessel function of first kind and order $n - n'$. The asymptotic distribution $P_s(n)$, shown in Fig. 2(a), is attained because the phases α of the nonresonant Bloch components of the original wave packet, accumulated under the action of the time evolution operator, are effectively averaged.

For finite times, $P(n, N)$ exhibits a narrow, stationary peak centered around $n = 0$, algebraic decay $\propto n^{-2}$ over intermediate momenta, and “ballistic wings” due to the almost-resonant β values, which move to higher momenta linearly in time. It is important to note that the central peak is narrower than the exponential distribution observed in dynamically localized atomic ensembles, and that the linear energy growth is observed at all times, in spite of the onset of the stationary distribution. There is no inconsistency here: the asymptotic limit to which the distribution tends has an n^{-2} fall-off at large n , and hence has an infinite mean energy (i.e., a divergent second moment). The ballistic wings, also experimentally observed in Ref. [11], dominate the theoretically computed mean energy growth. As the wings are fed by the resonant- β subclass, the resonant energy growth is ultimately due to conservation of the quasimomentum β in the kicking process.

Experimental detection of these wings in the final atomic momentum distribution is extremely difficult, for several reasons. The most important of these for our present discussion is that the wings must not have moved beyond the cutoffs imposed by the signal-to-noise ratio. Though relatively small

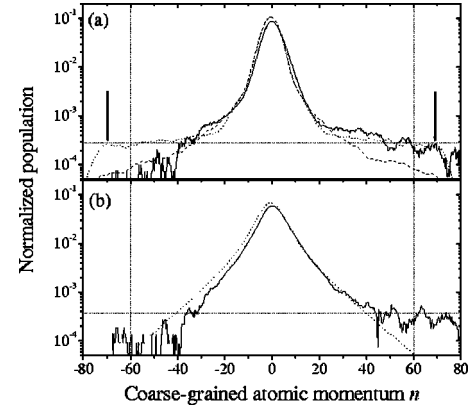


FIG. 2. Normalized experimental (solid line) and coarse-grained numerical (dotted line) momentum distributions after $N = 30$ kicks at the quantum resonance $\tau = 2\pi$ ($T = 66.5 \mu\text{s}$) in (a) the absence, and (b) the presence of induced spontaneous emission. Experimentally, $\bar{n}_{\text{SE}} = (0.14 \pm 0.04)$, while $\bar{n}_{\text{SE}} = 0.1$ numerically. The dashed curve in (a) is the asymptotic distribution $P_s(n)$, as given in Eq. (3). The arrow labels in (a) indicate the ballistic wings, whose momentum varies linearly with N . Note the slight asymmetry in the experimental distributions around $n = 0$, due to nonideal aspects of the realization. The fainter dotted lines show the signal threshold and momentum cuts imposed on the experimental data when calculating mean energies.

in terms of population, this experimental loss from the ballistic wings leads to a mean energy which is significantly less than the theoretical value. Our theoretical picture is compared with experimental data in Fig. 2(a), where experimental and numerical momentum distributions are shown at the quantum resonance $\tau = 2\pi$ ($T = 66.5 \mu\text{s}$), after $N = 30$ kicks. Note that our numerical simulation exhibits the ballistic wings of the distribution, which are swamped by the noise background in the experimental data. When processing such data, only momenta in the window $[-60, 60]$ were taken into account. Furthermore, the experimental distribution exhibits an asymmetry around $n = 0$ which is not present in the theory. This is due to two effects: the first, and most important, is that of the lock-in amplifier and its associated low pass filter, used in the TOF measurement, which slightly distort the momentum distribution. The second is that the removal of gravity’s effect by the crystal phase modulator is imperfect; gravity breaks the symmetry of the system’s evolution and hence of the momentum distribution. Nevertheless, the experimental and theoretical results agree very well in the central part of the distribution. Other deviations of the experimental system from the ideal are: (i) pulses are not δ -like as they have a finite duration t_p , (ii) random amplitude noise is introduced by laser power fluctuations ($\pm 5\%$), and (iii) different atoms are subject to somewhat different values of ϕ_d [12].

The addition of noise reshuffles the quasimomenta of the initial distribution, at a rate proportional to \bar{n}_{SE} , and thus destroys the conservation of quasimomentum. This reshuffling prevents atoms from remaining in the fast-traveling quasimomentum range for a long time; the formation of ballistic wings is thus inhibited. On the other hand, reshuffling gives all atoms a chance of sojourning a while in those qua-

simomentum ranges and hence experiencing a transient ballistic momentum growth. As a result, the distribution at moderate momenta broadens in time, at the expense of the ballistic wings. This is seen in Fig. 2(b): for $\bar{n}_{SE} \approx 0.14$, the momentum distribution is strongly broadened as it exhibits enhanced population of moderate momentum states.

The incoherent dynamics are amenable to analytical treatment [7], which shows that the distribution no longer approaches a stationary form. Instead, it evolves towards a continually broadening, diffusionlike Gaussian. The theoretically obtained line shape compares very favorably to the experimental one, as shown in Fig. 2(b). Note that we chose $\bar{n}_{SE} = 0.1$ for the analysis in order to achieve an optimal fit to the experimental data. The uncertainty in the intensity of $D2$ light experienced by the atoms, due to loss at the glass faces of the vacuum system and the exact shape of the $2 \mu\text{s}$ pulse, means that the experimental value of \bar{n}_{SE} is (0.14 ± 0.04) , consistent with this best theoretical fit.

Analytically, the mean energy grows according to $E \approx (D/2 + \phi_d^2/4)N$, where $D = \bar{n}_{SE}/12$ is the diffusion coefficient associated with the momentum transfer due to SE [7]. Since D is rather small (≈ 0.01) for the cases considered here, the mean energy growth is almost the same as in the resonant case *without* decoherence, where the same expression for E is obtained, except $D = 0$ (see above). Hence weak decoherence destroys the conservation of quasimomentum, which lies at the very root of resonances, yet in the ideal model it only affects the resonant energy growth mildly. However, the theoretically almost identical energy growth is produced by quite different physical mechanisms, which react to the cutoffs inherent in experimental detection schemes in dramatically different ways. In the coherently evolved

case, the growth of the experimentally measured energy is strongly depressed as soon as the ballistic wings escape the detection windows. In the presence of noise, the energy growth is not due to the *ballistic* wings, but rather to *diffusive* broadening of the whole distribution, and is therefore dominated by the center. Hence the effect of finite experimental detection windows is much less severe and the measured mean energy remains closer to its ideal value up to a higher value of N . This leads to an apparent enhancement of the resonance peaks compared to the SE-free case. Such noise-induced signal enhancement is reminiscent of “stochastic resonance,” where the response of a system to some input signal is enhanced by stochastic activation [17]. However, the hallmark of stochastic resonance is a maximum signal enhancement at an optimal, nonvanishing noise level. This has not so far been established in our present scenario.

In summary, we have shown that the linear growth with time of the mean energy at quantum resonance, inhibited in experiments by finite detection windows on finite time scales, is restored there by adding noise. This effect is ultimately rooted in the difference between atoms and rotors and is a striking, albeit indirect, demonstration of the peculiar nature of coherent resonant transport for kicked atoms, and how it is modified by photon recoil-induced decoherence.

We thank S.A. Gardiner and K. Burnett for stimulating and enlightening discussions. We acknowledge support from the U.K. EPSRC, The Royal Society, the EU TMR “Cold Quantum Gases” network and QTRANS RTN1-1999-08400, the INFM-PA project *Weak Chaos: Theory and Applications*, the U.S.-Israel Binational Science Foundation (BSF), and the Minerva Center of Nonlinear Physics of Complex Systems.

-
- [1] M. Greiner *et al.*, Nature (London) **415**, 39 (2002); O. Morsch *et al.*, Phys. Rev. Lett. **87**, 140402 (2001).
- [2] D. Jaksch *et al.*, Phys. Rev. Lett. **82**, 1975 (1999).
- [3] T. Dittrich and R. Graham, Z. Phys. B: Condens. Matter **62**, 515 (1986); D. Cohen, Phys. Rev. A **44**, 2292 (1991); R. Blümel *et al.*, *ibid.* **44**, 4521 (1991).
- [4] H. Ammann *et al.*, Phys. Rev. Lett. **80**, 4111 (1998).
- [5] *Coherent Evolution in Noisy Environments*, edited by A. Buchleitner and K. Hornberger, Springer Lecture Notes in Physics, Vol. 611 (Springer-Verlag, Berlin, 2002).
- [6] M.B. d’Arcy *et al.*, Phys. Rev. Lett. **87**, 074102 (2001).
- [7] S. Wimberger, I. Guarneri, and S. Fishman, Nonlinearity **16**, 1381 (2003).
- [8] F.M. Izrailev and D.L. Shepelyansky, Dokl. Acad. Nauk SSSR **249**, 1103 (1979) [Sov. Phys. Dokl. **24**, 996 (1979)].
- [9] S. Fishman, in *Quantum Chaos*, Proceedings of the International School of Physics “Enrico Fermi,” Course CXIX, edited by G. Casati, I. Guarneri, and U. Smilansky (IOS Press, Amsterdam, 1993).
- [10] P.W. Anderson, Phys. Rev. **109**, 1498 (1958).
- [11] W.H. Oskay *et al.*, Opt. Commun. **179**, 137 (2000).
- [12] M.B. d’Arcy *et al.*, Phys. Rev. E **64**, 056233 (2001).
- [13] R. Graham, M. Schlautmann, and P. Zoller, Phys. Rev. A **45**, R19 (1992); F.L. Moore *et al.*, Phys. Rev. Lett. **75**, 4598 (1995).
- [14] H.-J. Stöckmann, *Quantum Chaos: An Introduction* (Cambridge University Press, Cambridge, 1999).
- [15] A.L. Lichtenberg and M.A. Leiberman, *Regular and Chaotic Dynamics* (Springer-Verlag, Berlin, 1992).
- [16] D.L. Shepelyansky, Physica D **28**, 103 (1987).
- [17] A. Bulsara and L. Gammaitoni, Phys. Today **49**(3), 39 (1996); K. Wiesenfeld, T. Wellens, and A. Buchleitner, in *Coherent Evolution in Noisy Environments* (Ref. [5]).